

Polaron transport in the paramagnetic phase of electron-doped manganites

J. L. Cohn,¹ C. Chiorescu,¹ and J. J. Neumeier²

¹*Department of Physics, University of Miami, Coral Gables, Florida 33124, USA*

²*Department of Physics, Montana State University, Bozeman, Montana 59717, USA*

(Received 18 January 2005; published 13 July 2005)

The electrical resistivity, Hall coefficient, and thermopower as functions of temperature are reported for lightly electron-doped $\text{Ca}_{1-x}\text{La}_x\text{MnO}_3$ ($0 \leq x \leq 0.10$). Unlike the case of hole-doped ferromagnetic manganites, the magnitude and temperature dependence of the Hall mobility (μ_H) for these compounds is found to be inconsistent with small-polaron theory. The transport data are better described by the Feynman polaron theory and imply intermediate coupling ($\alpha \approx 5.4$) with a band effective mass $m^* \sim 4.3m_0$ and a polaron mass $m_p \sim 10m_0$.

DOI: [10.1103/PhysRevB.72.024422](https://doi.org/10.1103/PhysRevB.72.024422)

PACS number(s): 75.47.Lx, 71.38.-k, 72.20.-i

I. INTRODUCTION

Studies of perovskite manganites have drawn considerable attention to the issue of electronic phase separation as a paradigm for understanding strongly correlated electron systems generally.¹ Inhomogeneous magnetic ground states, observed over a broad range of compositions, are thought to arise from inhomogeneous paramagnetic (PM) states as a consequence of competing interactions. In the case of hole-doped, ferromagnetic colossal magnetoresistance (CMR) manganites, there exists compelling evidence that the PM phase is small-polaronic,²⁻⁴ and inhomogeneous due to local ferromagnetic (FM) and charge-order fluctuations.

Lightly electron-doped manganites, such as $\text{Ca}_{1-x}\text{La}_x\text{MnO}_3$, are structurally simpler than their hole-doped counterparts since cooperative Jahn-Teller distortions are largely absent due to the tetravalent state of most Mn ions. Antiferromagnetic (AF) superexchange interactions are dominant and dictate a G-type AF ground state for CaMnO_3 below $T_N = 125$ K. Electron doping⁵⁻⁸ via substitution of trivalent ions for Ca induces a weak FM moment associated with an inhomogeneous magnetic state.⁹

Transport properties in the PM phase of electron-doped manganites differ substantially from those of hole-doped FM compositions and consensus about the conduction mechanism is lacking. Both the resistivity and thermopower are thermally activated in hole-doped compounds in a manner consistent with a thermally activated mobility and small polaron theory. In contrast, the resistivity of lightly electron-doped compounds exhibits a positive temperature coefficient at $T \geq 150$ –200 K, and the thermopower decreases with decreasing T .⁵⁻⁸ The binding energy of small polarons, inferred from transport, decreases with increasing hole concentration,^{3,10} suggesting the possibility of a qualitative change in the character of polarons for electron-doped compositions.

The present paper focuses on charge carrier transport (resistivity, Hall effect, thermopower) near T_N and above in $\text{Ca}_{1-x}\text{La}_x\text{MnO}_3$ with the goal of clarifying the role and nature of polarons in the PM phase of electron-doped materials. The Hall mobility, which has not been previously reported for such compositions, is found to favor a large (continuum) rather than a small-polaron picture. Analysis of both the mo-

bility and thermopower imply intermediate coupling, with an electron-phonon coupling parameter $\alpha \approx 5.4$, an electron effective mass $m^* \sim 4.3m_0$, and a polaron mass $m_p \approx 10m_0$.

II. EXPERIMENT

Polycrystalline specimens of $\text{Ca}_{1-x}\text{La}_x\text{MnO}_3$ ($x \leq 0.10$) were prepared by solid-state reaction as described elsewhere.⁶ Powder x-ray diffraction revealed no secondary phases and iodometric titration, to measure the average Mn valance, indicated an oxygen content within the range 3.00 ± 0.01 for all specimens. The magnetization⁶ and thermal conductivity¹¹ of similar specimens have been described previously. A single crystal was grown from two polycrystalline rods of CaMnO_3 that were melted in a dual-mirror optical image furnace; one acted as a seed, the other was the feed rod. Both rods were rotated in opposing directions at 50 rpm during the growth and the rods moved downward at 5 mm/h through the hot zone. The heating power was 560 W and the growth was conducted in 2 atm. oxygen. Small single crystals a few millimeters in length were cut from the recrystallized rod. Resistivity, Hall, and thermopower (TEP) measurements were performed on all polycrystalline specimens; resistivity and TEP only for the crystal. The TEP was measured using a steady-state technique employing a fine-wire chromel-constantan thermocouple and gold leads. DC Hall and resistivity measurements were performed in separate experiments on six-probe Hall-bar specimens of approximate dimensions $1 \times 3 \times 0.15$ mm³ in a 9 T magnet; both current and field reversal were employed in the Hall measurements.

III. RESULTS

Figure 1 shows the electrical resistivity versus temperature for all of the compounds. The magnitude of ρ decreases systematically with doping. Specimens with $0.005 \leq x \leq 0.04$ exhibit a positive temperature coefficient of resistivity for $T > 200$ K. Similar qualitative features have been reported for electron doping with other lanthanides.^{6,8,9}

The Hall voltage, shown at $T = 250$ K for several compositions in Fig. 2(a), was negative (electronlike) and linear

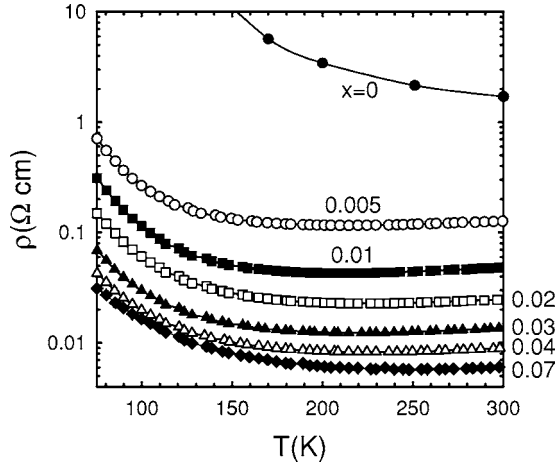


FIG. 1. Resistivity versus temperature for $\text{Ca}_{1-x}\text{La}_x\text{MnO}_3$. Data for $x=0.10$ are omitted for clarity.

in field for all specimens and temperatures in the PM phase. The Hall coefficient was computed as, $R_H = [dV_H/d(\mu_0 H)](t/I)$, where t is the specimen dimension along the field and I the current. Figure 2(b) shows the Hall number $n_H = V_{f.u.}/R_H|e|$, as a function of doping at $T = 250$ K. $V_{f.u.}$ was taken as $(205/4) \text{ \AA}^3$ for all x since variations in the cell volume⁹ over this range of doping constitute variations in n_H smaller than the measurement accuracy. It is seen that $n_H = -x$ is well obeyed, confirming that La doping adds approximately x electrons per formula unit. A value of $n_H = 0.01$ corresponds to a carrier density of $\approx 2 \times 10^{20} \text{ cm}^{-3}$.

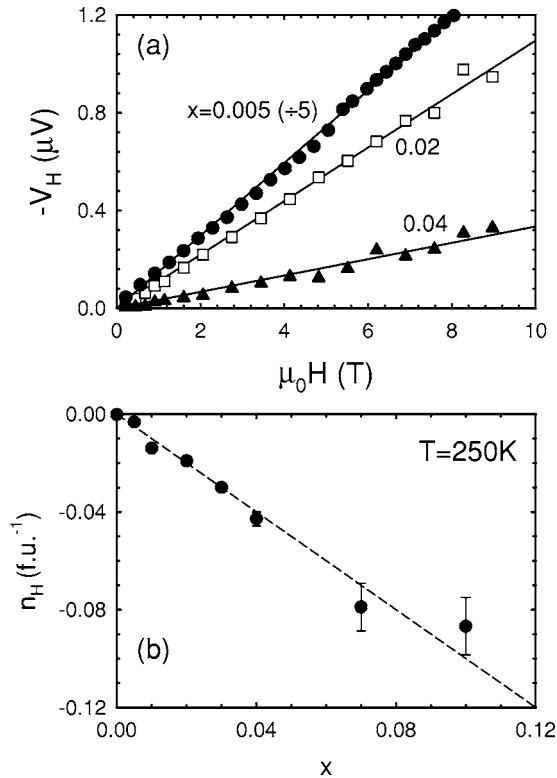


FIG. 2. (a) Hall voltage versus magnetic field and (b) Hall number versus x at $T=250$ K.

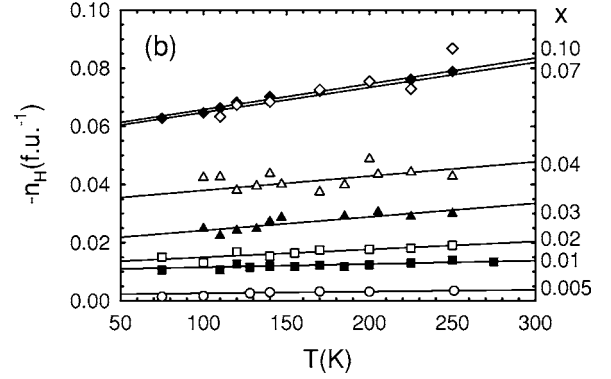
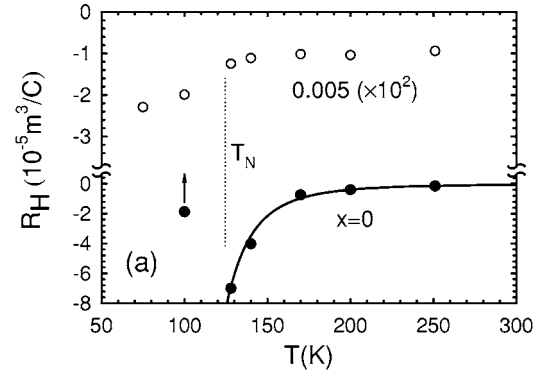


FIG. 3. (a) $R_H(T)$ for $x=0, 0.005$. The solid curve is an exponential fit (see text). (b) $n_H(T)$ for $x \geq 0.005$ with linear- T fits (solid lines).

$R_H(T)$ has an exponential dependence for $x=0$ in the PM phase with activation energy $E_H/k_B \sim 1000$ K [Fig. 3(a); the solid curve corresponds to $n_H = -1.25 \times 10^{-2} \exp(-1010/T)$]. Below $T_N \approx 125$ K, R_H turns sharply toward a positive value at 75 K corresponding to $n_H \approx 4 \times 10^{-8}$ (this was the lowest T for which R_H for $x=0$ could be reliably measured). This indicates partial compensation by a small density of holes. A small oxygen vacancy concentration is a likely source of electrons in CaMnO_3 , but a distribution of donors and acceptors is common in oxides. A smaller concentration of acceptors in the present compounds is expected to arise from several ppm levels of impurities (e.g., Al, Zn) in the starting chemicals. A smaller feature at T_N is observed for the $x=0.005$ specimen: An increase in $|R_H|$ with no sign change [Fig. 3(a)]. The $x=0.005$ specimen is degenerately doped with electrons so the behavior of R_H implies a decrease of the mobile electron concentration at $T < T_N$. The Hall coefficient in the presence of both mobile electrons (n) and holes (p) is expressed as $R_H = (1/e)(n\mu_n^2 - p\mu_p^2)/(n\mu_n + p\mu_p)^2$, where μ_n and μ_p are the electron and hole mobilities, respectively. Evidently as n is suppressed below T_N , the holelike contribution predominates in the $x=0$ specimen. No measurable effects are detected upon crossing T_N in $n_H(T)$ for the other La-doped specimens [Fig. 3(b)]. Their weak T dependencies for n_H are typical of degenerately doped semiconductors, and obey the empirical relation $n_H = A + BT$ [solid lines, Fig. 3(b)].

The Hall mobilities, $\mu_H \equiv R_H/\rho$ for all specimens are plotted in Fig. 4, where the fits from Fig. 3 have been employed

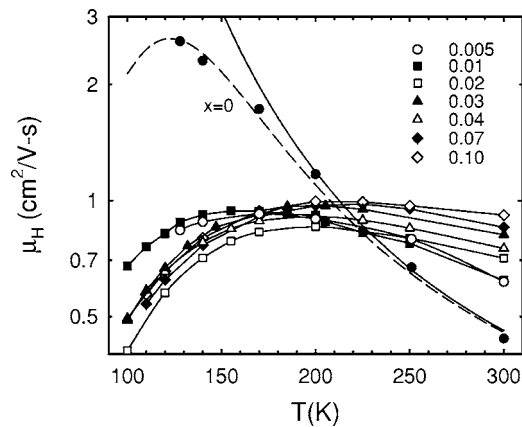


FIG. 4. $\mu_H(T)$ for all compositions in semilog scaling. The solid curve for $x=0$ represents Feynman polaron theory with phonon energy $\Theta=700$ K and $m^*=4.3m_0$ (see text). The dashed curve is a fit using the same polaron parameters with an additional term for impurity scattering (see text). The curves for doped specimens are guides to the eye.

to produce smoothed results. In general, μ_H determined from polycrystalline specimens should be viewed as a lower bound on intrinsic behavior, given that grain-boundary scattering tends to increase ρ , but has little effect on R_H even for highly anisotropic materials.¹² However our single crystal of CaMnO_3 , with a carrier density estimated from the TEP (see below) to be between that of the $x=0$ and $x=0.005$ polycrystalline specimens, had a room-temperature resistivity of $2.7 \Omega \text{ cm}$, somewhat larger than that of the $x=0$ polycrystal and implying a lower value for μ_H . Thus grain-boundary scattering appears to be relatively insignificant in determining the behavior of μ_H .

$\mu_H(T)$ increases strongly with decreasing temperature for $x=0$ from a room-temperature value of $\mu_H \approx 0.5 \text{ cm}^2/\text{V s}$ (Fig. 4). The doped specimen mobilities increase more weakly with decreasing temperature, reach maxima in the range 150–200 K, and decrease at lower temperatures. The qualitative features of the data are typical of polar semiconductors, with an intrinsic regime associated with phonon scattering at high T and an extrinsic region controlled by charged impurity scattering (particularly for the doped specimens) at low T . The weak, systematic increase in μ_H with doping at high T (Fig. 5) suggests another mechanism, discussed further in the next section. The overall magnitude $\mu_H \sim 1 \text{ cm}^2/\text{V s}$ at 200 K, is nearly two orders of magnitude larger than that of hole-doped FM compositions² and the small-polaron hopping mobility for the latter [$\mu_H \propto \exp(-E/k_B T)$], contrasts with the behavior observed here.

Thermoelectric power data are shown in Fig. 6. The TEP for $x=0$ is $\sim -550 \mu\text{V}/\text{K}$ at room temperature and grows larger with decreasing T , consistent with the presence of an activation energy as indicated by the behavior of $\rho(T)$ and $n_H(T)$. With increasing x the TEP is reduced in magnitude and has a T dependence typical of degenerately doped semiconductors.¹³ The overall features are similar to observations on Sm- and Pr-doped CMO.^{5,7} The TEP behavior for the doped specimens contrasts with the thermally activated ($S \propto 1/T$) behavior that typifies the PM-phase TEP of hole-doped, FM compounds.^{2,3,14}

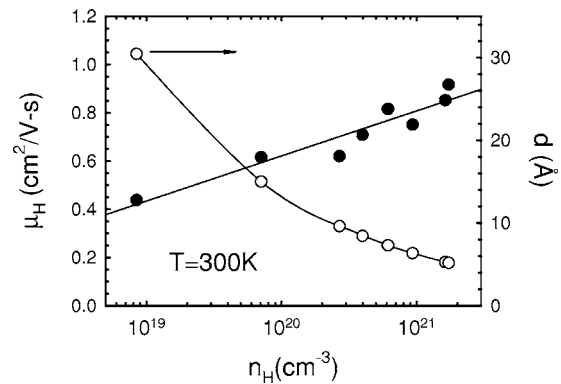


FIG. 5. μ_H (solid circles) and mean dopant spacing (open circles, right ordinate) versus Hall carrier density at room temperature. Curves are guides to the eye.

The TEP magnitude for all specimens increases abruptly at $T < T_N$. This is attributed to a reduction in electron transfer (via double exchange) as the majority of Mn core spins take on an AF arrangement. The corresponding reduction in the mobile electron concentration enhances the TEP magnitude, in agreement with our observations above regarding the Hall coefficient. We also note that small features at T_N , consistent with a decrease in carrier concentration and/or mobility, are evident in the temperature derivatives of the $\rho(T)$ curves.

For all of the doped specimens, the TEP tends toward zero as $T \rightarrow 0$, indicating a finite density of states at the Fermi level. This is consistent with prior low- T resistivity⁶ and ac impedance measurements¹⁵ which suggest that the Fermi level lies in a disorder-broadened impurity “band” close in energy to the band edge.

IV. ANALYSIS AND DISCUSSION

A strong interaction between carriers and optical phonons typifies perovskite oxides. As noted above, the magnitude

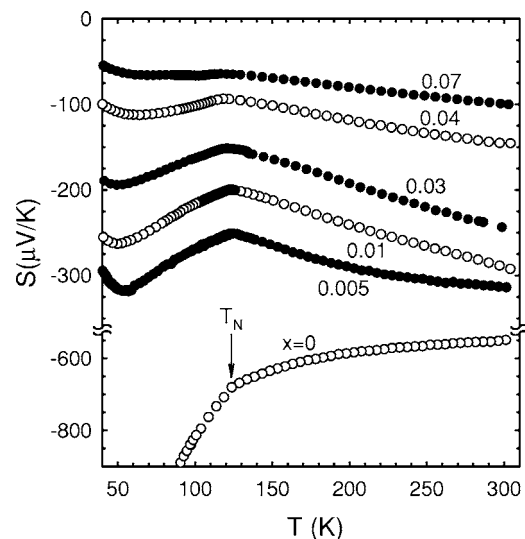


FIG. 6. Thermopower versus temperature. Data for $x=0.02$ and 0.10 are omitted for clarity.

and temperature dependence of both μ_H and the TEP argue against the use of small (Holstein) polaron theory which has been successful in describing hole-doped manganites. Nevertheless, a large static dielectric constant¹⁵ $\epsilon_0 \approx 40$, determined for similarly prepared CaMnO_3 , makes polaron formation likely in electron-doped compounds given that the optical-frequency dielectric constant for manganites (and oxides generally)¹⁶ is substantially smaller, $\epsilon_\infty \approx 5$. These observations motivate a Fröhlich (continuum or large) polaron description for the charge carriers in this system. Before analyzing the data, it is useful to estimate the dimensionless polaron coupling constant¹⁷

$$\alpha = 397.4 \left[\frac{(m^*/m_0)}{\Theta} \right]^{1/2} (\epsilon_\infty^{-1} - \epsilon_0^{-1}),$$

where m^* is the band mass (without polaron enhancement), m_0 the free-electron mass, $\Theta = \hbar\omega_0/k_B$, and ω_0 the longitudinal optic (LO) phonon frequency. Taking $\Theta \sim 700$ K as an average LO phonon energy,¹⁸ and $m^* = m_0$ implies $\alpha \sim 2.6$. The donor binding energy and dielectric constant of CaMnO_3 suggest¹⁵ $m^* \sim 4m_0$ and thus a proper treatment of the transport properties requires a theory suitable for intermediate coupling ($2 \leq \alpha \leq 6$).

The most reliable theory for large polaron mobility at intermediate coupling and intermediate temperatures ($T \lesssim \Theta$) is that of Feynman *et al.*¹⁹ The polaron mobility is given (in $\text{cm}^2/\text{V s}$) as²⁰

$$\mu_p = \frac{7.14 \times 10^4}{\alpha \Theta} \left(\frac{m_0}{m^*} \right) \frac{\sinh(z/2) w^3}{(z/2)^{5/2} v^3 K(v, w, z)},$$

where $z = \Theta/T$. The integral $K(v, w, z)$ and the procedure for determining the Feynman variational parameters v and w at each temperature for a given value of m^*/m_0 are described in Ref. 20. The mobility data at the highest temperatures for $x=0$ were fitted using $\Theta = 700$ K and $m^*/m_0 = 4.3$ ($\alpha \approx 5.4$) [solid curve in Fig. 4]. The discrepancy between experiment and theory below 175 K is plausibly attributed to the growing role of impurity scattering with decreasing T . To fit the entire T range, μ_p was combined with the Brooks-Herring mobility²¹ for charged impurity scattering (in $\text{cm}^2/\text{V s}$),

$$\mu_{\text{BH}} = \frac{3.68 \times 10^{20} \text{ cm}^{-3}}{N_I} \frac{1}{Z^2} \left(\frac{\epsilon_0}{16} \right)^2 \left(\frac{T}{100 \text{ K}} \right)^{3/2} \left(\frac{m_0}{m^*} \right)^{1/2} f(\beta),$$

$$f(\beta) = [\ln(1 + \beta^2) - 0.434\beta^2/(1 + \beta^2)]^{-1},$$

$$\beta = \left(\frac{\epsilon_0}{16} \right)^{1/2} \left(\frac{T}{100 \text{ K}} \right) \left(\frac{m^*}{m_0} \right)^{1/2} \left(\frac{2.08 \times 10^{18} \text{ cm}^{-3}}{n} \right)^{1/2}.$$

The dashed curve through the $x=0$ mobility (Fig. 4) represents $\mu = (\mu_p^{-1} + \mu_{\text{BH}}^{-1})^{-1}$, using $n = n_H(T)$, $Z=2$ (for oxygen vacancies), $\epsilon_0 = 40$, and $m^*/m_0 = 4.3$. The impurity concentration (the remaining free parameter) required to fit the data was $N_I = 3 \times 10^{19} \text{ cm}^{-3}$, roughly four times the $T=300$ K Hall carrier concentration. A similar discrepancy was observed²² for the impurity term describing the mobility of $\text{La}_2\text{CuO}_{4+y}$. The disagreement is reasonable considering that only the charge difference associated with the oxygen vacancy, but

not the lattice distortion, is considered in the Brooks-Herring theory. Long-ranged, correlated disorder is an important characteristic²³ of the perovskite oxides due to the corner-sharing metal-oxygen polyhedra.

Let us briefly discuss the polaron mass and size dictated by this analysis. The Feynman polaron mass at room temperature is $m_p = (v/w)^2 m_0 \approx 36m_0$. The Feynman path integral theory gives a larger effective mass than other approaches to the problem and a reasonable lower bound on the mass is given by the perturbation theory result, shown to be a good approximation even for intermediate coupling,²⁴ $m_p = m^*(1 + \alpha/6) \approx 8.4m_0$. The Feynman polaron radius is given as,²⁵ $R_p = (3\hbar/2\mu v)^{1/2} \approx 3 \text{ \AA}$ [$\mu = m^*(v^2 - w^2)/v^2$], comparable to a lattice spacing. Thus the continuum approximation is near its limit of validity. This value of R_p is consistent with the seven-site FM polaron predicted for the magnetically ordered ($T=0$) state of CaMnO_3 from theoretical studies^{26,27} incorporating both lattice and spin interactions. Magnetic contributions to PM-phase polaron formation are presumably less significant than that of the lattice, though it has been proposed that magnetic fluctuations increase the polaron binding energy, yielding low-mobility magnetoelastic polarons for lower electron-phonon coupling strengths.²⁸ The latter effects could possibly contribute to the downturn in the mobility modeled above by charged impurity scattering.

The simple sum of scattering mechanisms describing $\mu_H(T)$ for $x=0$ is inadequate for the doped specimens, given the systematic increase in μ_H with doping at high T (Fig. 5). The enhanced mobility might signify the effects of overlapping polaronic lattice distortions. If so, the mean distance between dopants $d = (3/4\pi n)^{1/3}$ (n is the carrier density) plotted in Fig. 5 (open circles), suggests that the distortion field extends over a few lattice spacings. Low- T magnetization⁶ and neutron scattering⁹ studies suggest a crossover near $x=0.02$ from isolated to interacting FM polarons.

The TEP offers an alternative, though less reliable, means for assessing the effective mass. We are not aware of a theory for the TEP valid for intermediate coupling, but the weak-coupling (perturbative) theory of Howarth and Sondheimer (HS)²⁹ was found to provide a good description of the TEP. It is known that weak coupling theories tend to overestimate the band effective mass. A heuristic approach, wherein the band mass within weak-coupling theories is interpreted as the polaron-enhanced mass, has been proposed to broaden their range of applicability.³⁰ We restrict our analysis to the doping dependence of the TEP at room temperature where optical phonon scattering is predominant. Though the HS theory reproduces the T dependence of the TEP well, such an analysis is less meaningful given that the theory does not incorporate impurity scattering (of growing importance for the present compounds at low T) or a temperature dependent polaron mass (implicit in Feynman theory).

The HS theory gives the TEP as a function of the phonon energy (Θ) and reduced chemical potential.³¹ With $\Theta = 700$ K and the chemical potential determined self-consistently from the Hall carrier density (assuming a parabolic band), the TEP can be computed with the effective mass (designated here as m^{**}) as the only adjustable param-

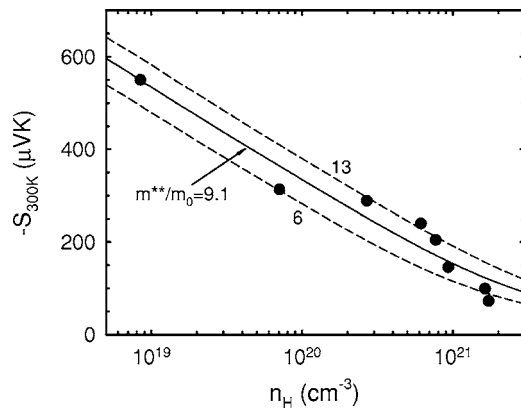


FIG. 7. Room-temperature thermopower versus Hall carrier density. The solid and dashed curves were computed using the theory of Ref. 29, with effective masses indicated (see text).

eter. Figure 7 shows the room temperature TEP plotted versus Hall carrier density for all specimens. The solid curve represents the best fit to the HS theory with $m^{**}=9.1m_0$. Variations in the polaron mass with doping might possibly explain the discrepancy between the calculated and measured TEP magnitudes (corresponding to variations in m^{**}/m_0 from 6 to 13, indicated by dashed curves), but these differences may simply reflect a sensitivity of the TEP to extrinsic features, e.g., small variations in the oxygen vacancy concentration (below the uncertainty of 0.01 per f.u. from titration), that cause it to deviate from being a monotonic function of the carrier density as reflected in the Hall coefficient. Thus the polaron masses determined from μ_H and the TEP are in reasonable accord.

It is useful to place in context the intermediate-coupling, Fröhlich polaron picture for the PM phase of electron-doped manganites favored by the present analysis. Recently, polaron parameters were inferred from pressure-dependent resistivity measurements³² on $\text{Ca}_{1-x}\text{Y}_x\text{MnO}_3$ ($0.05 \leq x \leq 0.15$) having $\rho(T)$ very similar to that of the most heavily doped specimens in Fig. 1. These authors interpreted the minimum

in $\rho(T)$ (near $T=200$ K in Fig. 1) as a manifestation of the crossover from the intermediate- T small-polaron regime, characterized by thermally activated hopping, to the high- T regime where polarons are thermally dissociated and phonon scattering of residual electrons yields a positive temperature coefficient of ρ .^{33,34} Analyzing the pressure dependence of the activation energy from $\rho(T)$ over the narrow T interval between T_N and the minimum, they inferred a coupling strength, $\alpha \approx 1.5$. The strongest argument against this interpretation is that the minimum in $\rho(T)$ arising in small polaron theory occurs at several times the optical phonon energy (Θ), well above the temperature range investigated. In addition, as noted above, polarons with activated $\rho(T)$ are expected to exhibit an activated TEP ($\propto 1/T$), inconsistent with the present observations and those of others.^{5,7}

The electron-doped manganite compounds are evidently near a large- to small-polaron crossover. A comparable situation arises in TiO_2 (rutile), for which $\mu_H(T)$ and $\rho(T)$ are similar to data for the present materials and both small^{24,35,36} and large^{37,38} polaron descriptions have been invoked. Recent measurements of the Hall mobility by an all-optical technique³⁸ support a continuum picture for that system, like that described here. The appropriate theoretical framework for describing such materials remains an active area of investigation,^{28,34,39,40} and the electron-doped compounds appear to be model systems for studying polaron physics.

In summary, the PM-phase Hall mobility and thermopower of $\text{Ca}_{1-x}\text{La}_x\text{MnO}_3$ ($0 \leq x \leq 0.10$) and other lightly electron-doped manganites by implication, are consistent with large (continuum) polaron theory in the intermediate coupling regime. This behavior is distinguished from the small-polaron scenario that has been successful in describing the PM phase of hole-doped FM manganites.

ACKNOWLEDGMENTS

The work at the University of Miami was supported by NSF Grant No. DMR-0072276, and at Montana State University by Grant No. DMR-0301166.

¹E. Dagotto, T. Hotta, and A. Moreo, Phys. Rep. **344**, 1 (2001).
²M. Jaime, H. T. Hardner, M. B. Salamon, M. Rubinstein, P. Dorsey, and D. Emin, Phys. Rev. Lett. **78**, 951 (1997).
³J. L. Cohn, J. Supercond. **13**, 291 (2000).
⁴M. B. Salamon and M. Jaime, Rev. Mod. Phys. **73**, 583 (2001).
⁵A. Maignan, C. Martin, F. Damay, B. Raveau, and J. Hejtmanek, Phys. Rev. B **58**, 2758 (1998).
⁶J. J. Neumeier and J. L. Cohn, Phys. Rev. B **61**, 14319 (2000).
⁷C. Martin, A. Maignan, M. Hervieu, B. Raveau, Z. Jirak, M. Savosta, A. Kurbakov, V. Trounov, G. Andr, and F. Boure, Phys. Rev. B **62**, 6442 (2000); M. M. Savosta, P. Novak, M. Marysko, Z. Jirk, J. Hejtmanek, J. Englich, J. Kohout, C. Martin, and B. Raveau, *ibid.* **62**, 9532 (2000).
⁸H. Aliaga, M. T. Causa, M. Tovar, and B. Alascio, Physica B **320**, 75 (2002); H. Aliaga, M. T. Causa, B. Alascio, H. Salva, M. Tovar, D. Vega, G. Polla, G. Leyva, and P. Konig, J. Magn.

Magn. Mater. **226–230**, 791 (2001).

⁹C. D. Ling, E. Granado, J. J. Neumeier, J. W. Lynn, and D. N. Argyriou, Phys. Rev. B **68**, 134439 (2003); E. Granado, C. D. Ling, J. J. Neumeier, J. W. Lynn, and D. N. Argyriou, *ibid.* **68**, 134440 (2003).
¹⁰J. M. De Teresa, K. Dörr, K. H. Müller, L. Schultz, and R. I. Chakalova, Phys. Rev. B **58**, R5928 (1998).
¹¹J. L. Cohn and J. J. Neumeier, Phys. Rev. B **66**, 100404 (2002).
¹²Ting-Kang Xia and D. Stroud, Phys. Rev. B **37**, 118 (1988).
¹³G. A. Slack and M. H. Hussain, J. Appl. Phys. **70**, 2694 (1991).
¹⁴M. Jaime, M. B. Salamon, M. Rubinstein, R. E. Treece, J. S. Horwitz, and D. B. Chrisey, Phys. Rev. B **54**, 11914 (1996).
¹⁵J. L. Cohn, M. Peterca, and J. J. Neumeier, Phys. Rev. B **70**, 214433 (2004).
¹⁶A. S. Alexandrov and A. M. Bratkovsky, J. Phys.: Condens. Matter **11**, L531 (1999).

- ¹⁷See, e.g., K. Seeger, *Semiconductor Physics* (Springer-Verlag, Berlin, 1997), p. 209.
- ¹⁸L. Kebin, L. Xijun, Z. Kaigui, Z. Jingsheng, and Z. Yuheng, *J. Appl. Phys.* **81**, 6943 (1997); M. V. Abrashev, J. Bäckstrom, L. Börjesson, V. N. Popov, R. A. Chakalov, N. Kolev, R.-L. Meng, and M. N. Iliev, *Phys. Rev. B* **65**, 184301 (2002); L. Martín-Carrón, A. de Andrés, M. J. Martínez-Lope, M. T. Casais, and J. A. Alonso, *ibid.* **66**, 174303 (2002); N. N. Loshkareva, L. V. Nomerovannaya, E. V. Mostovshchikova, A. A. Makhnev, Y. P. Sukhorukov, N. I. Solin, Y. I. Arbutova, S. V. Naumov, N. V. Kostromitina, A. M. Balbashov, and L. N. Rybina, *ibid.* **70**, 224406 (2004).
- ¹⁹R. P. Feynman, *Phys. Rev.* **97**, 660 (1955); R. P. Feynman, R. W. Hellwarth, C. K. Iddings, and P. M. Platzman, *ibid.* **127**, 1004 (1962).
- ²⁰R. W. Hellwarth and I. Biaggio, *Phys. Rev. B* **60**, 299 (1999).
- ²¹K. Seeger, *Semiconductor Physics*, 6th ed. (Springer-Verlag, New York, 1997), Chap. 6; D. Chattopadhyay and H. J. Queisser, *Rev. Mod. Phys.* **53**, 745 (1981).
- ²²C. Y. Chen, E. C. Branlund, C. S. Bae, K. Yang, M. A. Kastner, A. Cassanho, and R. J. Birgeneau, *Phys. Rev. B* **51**, 3671 (1995).
- ²³J. Burgy, A. Moreo, and E. Dagotto, *Phys. Rev. Lett.* **92**, 097202 (2004).
- ²⁴A. S. Alexandrov and N. Mott, *Polarons and Bipolarons* (World Scientific, Singapore, 1995).
- ²⁵T. D. Schultz, *Phys. Rev.* **116**, 526 (1959).
- ²⁶Y.-R. Chen and P. B. Allen, *Phys. Rev. B* **64**, 064401 (2001).
- ²⁷H. Meskine, T. Saha-Dasgupta, and S. Satpathy, *Phys. Rev. Lett.* **92**, 056401 (2004).
- ²⁸E. L. Nagaev, *Phys. Rev. B* **60**, R6984 (2001).
- ²⁹D. J. Howarth and E. H. Sondheimer, *Proc. R. Soc. London, Ser. A* **219**, 53 (1953).
- ³⁰F. Garcia-Moliner, *Phys. Rev.* **130**, 2290 (1963).
- ³¹Equations (70)–(73) from Ref. 29 for the case of arbitrary degeneracy were employed.
- ³²G. Garbarino, C. Acha, D. Vega, G. Leyva, G. Polla, C. Martin, A. Maignan, and B. Raveau, *Phys. Rev. B* **70**, 014414 (2004).
- ³³J. Appel, in *Solid State Physics*, edited by F. Seitz, D. Turnbull, and H. Ehrenreich (Academic Press, New York, 1968), Vol. 21, pp. 193–391.
- ³⁴S. Fratini and S. Ciuchi, *Phys. Rev. Lett.* **91**, 256403 (2003).
- ³⁵V. N. Bogomolov, E. K. Kudinov and Yu A. Firsov, *Fiz. Tverd. Tela (Leningrad)* **9**, 3175 (1967).
- ³⁶E. Yagi, R. R. Hasiguti, and M. Aono, *Phys. Rev. B* **54**, 7945 (1996).
- ³⁷J. F. Baumard and F. Gervais, *Phys. Rev. B* **15**, 2316 (1977).
- ³⁸E. Hendry, F. Wang, J. Shan, T. F. Heinz, and M. Bonn, *Phys. Rev. B* **69**, 081101(R) (2004).
- ³⁹A. S. Alexandrov and P. E. Kornilovitch, *Phys. Rev. Lett.* **82**, 807 (1999).
- ⁴⁰C. A. Perroni, G. Iadonisi, and V. K. Mukhomorov, cond-mat/0411653 (unpublished).